FLT imaging systems for real-time FLT guidance

Van den Dries, T., Vrijsen J., Ingelberts H., Janssen S., de Rooster H., and Kuijk M.

Small literature overview in context of the FWO interdisciplinary grant submission: Enabling Wound Monitoring Through Real-time Fluorescence Lifetime Imaging with Novel Time-Gated Image Sensors.

Accurately observing the FLT is best done through measurements in the **time domain**. In this approach, the fluorescent agents are excited by a pulsed laser. One can deduce the agent's lifetime based on the course of the fluorescent light intensity over time. A typical scenario is depicted in Figure 1(a). In this simplified case, the fluorescent tracer follows first-order kinetics. Its lifetime (τ) is straightforwardly deduced from the mono-exponential decay. Note the faintness of the fluorescent emission due to the dyes' low quantum yield, extinction coefficient and the lack of directionality in fluorescent emission.

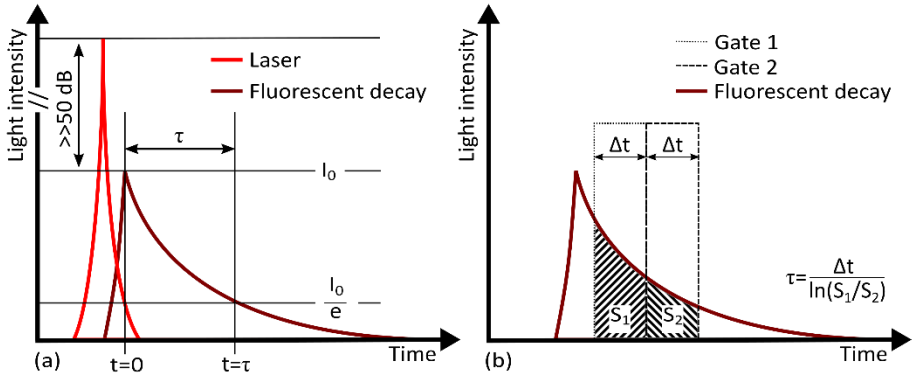

Figure 1: The FLT (τ) in the time domain. (a) Fluorescent emission decay caused by an excitation by a pulsed laser. (b) Lifetime calculation through time-gating and RLD. Adapted from [1].

Sub-nanosecond lifetimes and **very low fluorescent light intensities** are anticipated for FLGS [2]. To address this, the excitation source pulses at e.g. 50 MHz, allowing for many acquisitions per frame. A typical value for the resulting irradiance of the incoming fluorescent light is 1 $\frac{\mu W}{cm^2}$, translating to an average of 2.5 incoming photons per fluorescent decay for a 15µm x 15µm pixel. This evidently poses substantial demands on the time-resolved imaging system for FLT imaging.

The remainder of this section delves into state-of-the-art FLT imaging systems. It simultaneously highlights their strengths and the factors preventing them from enabling FLGS. The sensors' key specifications are also summarized in Table 1 (p. 4). It will be concluded that the **absence of an imager suited for FLGS persists** as a notable gap in current technology.

a. Intensified Charge-Coupled Devices (ICCDs)

Before the rise of CMOS Image Sensors (CISs) during the last two decades, most imaging systems used Charge-Coupled Devices (CCDs). The same is true for the original FLT imaging systems.

ICCDs for FLT imaging can be classified as **time-gated** image sensors. They estimate the lifetime by sampling the emitted fluorescent light in narrow time windows. Returning to the simplified example of a mono-exponential decay, the lifetime can be analytically determined using the intensity in two time windows, as depicted in Figure 1(b). This (over)simplified approach is known as Rapid Lifetime Determination (RLD)[1] [1], and serves well to illustrate the requirements on a sensor for FLGS.

[1] More complete FLT algorithms exist and are further being developed at our department and affiliated institutions, yet are out of scope for this project.

CCDs are intrinsically not able to discriminate in time between incoming photons. The time-resolvement is obtained by externally modulating the incoming light through an image intensifier placed before the CCD. Time-gating is then achieved by swiftly modulating the intensifier's gain.

However, the use of image intensifiers **limits the effective resolution** of ICCDs. Moreover, the few recent cameras whose minimum gate width is suitable for FLGS exhibit a **low quantum efficiency (QE) at NIR wavelengths** [3]. Gating the intensifiers's gain also introduces **excess noise** in the signal. Finally, the intensifiers are both fragile and expensive; the cost of an ICCD-based camera can be upwards of €100,000.

b. Single-Photon Avalanche Diodes (SPADs)

SPADs are detectors that generate a digital pulse to a **single incident photon**. They can determine the time-of-arrival of single photons with a picosecond time accuracy. Since the introduction of SPADs in low-cost CMOS processes, they have become the detector of choice in many demanding photonic applications.

A popular way of determining a fluorescent decay with SPADs is known as Time-Correlated Single Photon Counting (TCSPC) [4]. This technique logs the arrival time of subsequent photons in a histogram, which converges to the fluorescent decay over time. However, this requires large in-pixel circuits, which reduces the light-sensitive area of the pixel. As a result, the SPAD pixel's **fill factor (FF)**, the relative portion of the pixel's surface that is light-senstive, is typically little more than 10%. Combined with their shallow junctions, SPADs exhibit at NIR wavelengths a **limited Photon Detection Efficiency (PDE)**, which is the equivalent of the QE in the context of SPADs [5].

To increase the SPADs' FF, time-gated SPADs have been introduced as an alternative to TCSPC. For example, analog counting pixels can elevate the FF to 20% [6]. Research to increase the SPADs' PDE is also ongoing – including in our department. Charge-focusing SPADs are an interesting approach to overcome the existing hurdles [1] [7]. If this technique could be time-gated uniformly over the array, a high-resolution FLT imaging SPAD array could see the light of day.

c. Demodulating pixels (DMPs)

DMPs modulate photogenerated charges with an electric field. However, their originally used CCDs prove inadequate for swiftly capturing optical phenomena, as demanded in FLT imaging. Alternative topologies incorporating **pinned photodiodes (PPDs)** were devised for measuring the FLT.

The PPD is a pivotal element in many CISs. Its introduction mitigated all prevalent readout noise sources in CISs, catapulting them beyond the performance of classical CCDs. A PPD stores the photogenerated charges in a **buried diode**, termed the **storage well (SW)**, which eliminates dark current noise. Charge transfer from the SW to a **floating diffusion (FD)** occurs via a **transfer gate (TX)** after the FD is reset. Through clever readout strategies, PPDs allow for a readout noise as low as 1 electron (e^-) RMS. The advent of the low-noise CIS, coined the **scientific CMOS image sensor (sCIS)**, was a direct outcome of this innovation. DMPs are just one of PPDs' numerous applications, and its significance will also extend to this project.

DMPs incorporating PPDs achieve time-gating by connecting multiple TXs to one guide node. By enabling a maximum of one TX at a time, photogenerated charges are stored at the SW of interest. Each subsequent FD could be referred to as a **tap**; the number of taps typically ranges between two and eight [8].

To improve the QE at NIR wavelengths, charge focusing through a potential gradient in the substrate has been implemented. In a Back-Side-Illuminated (BSI) sensor, a high NIR sensitivity and FF are achievable [9]. However, the resulting prolonged traveling time for photogenerated carriers results in a **long intrinsic gating decay**, rendering it ill-suited for short NIR FLTs as needed for FLGS.

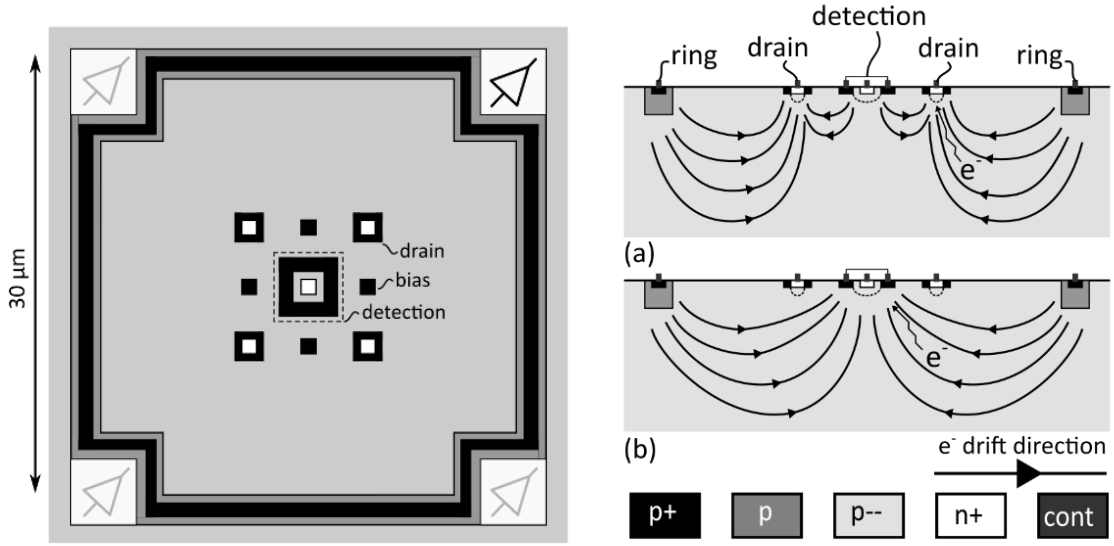

Figure 2: Left: top view of the CAPS pixel. Right: cross section of the CAPS pixel and doping levels; e^- drift direction when the gating signal is (a) low and (b) high. Adapted from [1].

d. Current-Assisted Photonic Sampler (CAPS)

Given the current state-of-the-art, there exists no sensor exhibiting both a high external QE (PDE in the context of SPADs) and a short intrinsic gating decay. For this reason, our group has developed the **Current-Assisted Photonic Sampler (CAPS)**. This novel type of image sensor achieves the same fast gating capabilities as intensified imagers, combined with a high QE at NIR wavelengths.

It meets these requirements through the current-assistance principle: an externally applied potential generates a majority current in the substrate, which allows to gather photogenerated electrons from deep within the substrate. The latest CAPS sensor shows an internal **QE of 46%** at 780nm and a **320ps intrinsic gating decay**. Other key properties of the latest CAPS pixel and its state-of-the-art competitors are listed in Table 1 (p. 4).

The CAPS pixel achieves its high contrast time-gating capabilities by modulating the substrate current. Figure 2 illustrates the pixel's top view and cross section in its two modes of operation: a differential gating signal is toggled between the **detection and drain node(s)**, which steers electrons from deep within the epilayer toward either of the nodes. This allows to discriminate incoming photons in time, effectively either detecting or draining their photogenerated charges.

However, the CAPS pixel still reveals some fundamental limitations. Its **readout noise** (67 e^- RMS) is particularly high, and its architecture intrinsically introduces **motion artefacts** in lifetime measurements. Hence, the current CAPS pixel needs a number of structural changes for it to be applied in FLGS.

Table 1: Specifications of state-of-the-art sensors for FLT imaging and the pursued pixel arrays in this project. The existing sensors' deficiencies for FLGS are highlighted in red.

	ICCD [3]	SPAD [5]	DMP [9]	CAPS [10]	CAPS RO1	CAPS RO2	CAPS RO3
Process	NA	180 nm CMOS	130 nm CMOS BSI	350 nm CMOS	180 nm CMOS	180 nm CMOS	180 nm CMOS
Pixel pitch (µm)	12.8	9.6	15	15	12	12	12
Resolution	256 x 256	500 x 500	41 x 41	160 x 120	320 x 240	640 x 480	640 x 480
FF	NA	10.5%	75%	62%	76%	70%	60%
NIR-I EQE / PDE	12%	1.5%	67.5%	29%	43%	40%	34%
Min. gate width (ns)	0.5	1	>15	1.5	1 (1 tap)	1 (1 tap)	1 (3 tap)
FR (fps)	26 (16 bit)	49800 (1 bit)	NA	60 (12 bit)	60 (12 bit)	30 (14 bit)	60 (14 bit)
Noise floor (e^- RMS)	16	0	NA	67	< 30	< 5	< 5

References

[1] G. Jegannathan, …, M. Kuijk, "An Overview of CMOS Photodetectors Utilizing Current-Assistance for Swift and Efficient Photo-Carrier Detection," *MDPI Sensors,* vol. 21, no. 13, pp. 4576-4603, 2021.

[2] R. Pal, …, A. T. N. Kumar, "Fluorescence Lifetime-Based Tumor Contrast Enhancement Using an EGFR Antibody-Labeled Near-Infrared Fluorophore," *Clinical Cancer Research,* vol. 25, no. 22, pp. 6653-6661, 15 November 2019.

[3] Teledyne Princeton Instruments, "PI-MAX®4," [Online]. Available: https://www.princetoninstruments.com/products/pi-max-family/pi-max. [Accessed 10 December 2023].

[4] J. R. Lakowicz, Principles of Fluorescence Spectroscopy, Springer, 2006.

[5] M. Wayne, …, E. Charbon, "A 500 × 500 Dual-Gate SPAD Imager With 100% Temporal Aperture and 1 ns Minimum Gate Length for FLIM and Phasor Imaging Applications," *IEEE Transactions on Electron Devices,* vol. 69, pp. 2865-2872, June 2022.

[6] M. Perenzoni, …, D. Stoppa, *IEEE Journal of Solid-State Circuits,* vol. 51, no. 1, pp. 155-167, 2016.

[7] K. Morimoto, …, T. Ichikawa, "3.2 Megapixel 3D-Stacked Charge Focusing SPAD for Low-Light Imaging and Depth Sensing," *IEEE International Electron Devices Meeting,* pp. 20.2.1-20.2.4, 2021.

[8] Y. Shirakawa, …, S. Kawahito, "An 8-Tap CMOS Lock-In Pixel Image Sensor for Short-Pulse Time-of-Flight Measurements," *MDPI Sensors,* vol. 20, no. 4, p. 1040, 2020.

[9] Y.-T. Chang, …, J. Lee, "Design and Characterization of Near-Infrared Sensitivity-Enhanced Three-Tap Fully Depleted Image Sensor for Fluorescence Lifetime Imaging," *IEEE Sensors,* vol. 22, pp. 18428-18436, October 2022.

[10] T. Van den Dries, *Image sensors to enable fluorescence lifetime guided surgery,* Brussels: Vrije Universiteit Brussel, 2023. PhD Thesis.